


ORIGINAL INNOVATION

Open Access



Methodology for calculating load capacity reduction and slip relationship of clustered group nail connectors

Shichao Wang^{1*} , Chenhao Tang¹, Yanqing Fu², Jianrui Zhu¹, Jianping Di¹ and Guodong Li³

*Correspondence:
wangshichao@chd.edu.cn

¹ School of Highway, Chang'an University, Xi'an 710064, China

² Central Research Institute of Building and Construction Co., Ltd. MCC Group, Beijing 100088, China

³ Institute of Transportation, Inner Mongolia University, Hohhot 010070, China

Abstract

Clustered group nail connectors are key connecting components for the full lifecycle construction and safe operation of steel–concrete composite structural bridges. To thoroughly investigate the stress mechanism of clustered group nail connectors in steel–concrete composite structures, this paper conducts a detailed numerical analysis on 100 sets of such connectors. It analyzes the stress mechanism of individual nail connectors and quantitatively calculates the group nail effect under the coupled action of multiple factors (nail spacing between layers, number of nail layers, concrete strength). Based on clarifying the force transmission patterns of nails and concrete in different layers during the loading process, this paper proposes a method for calculating the average bearing capacity reduction coefficient and the load-slip curve of single nails in clustered group nail connectors under the coupled action of multiple factors, which has been validated by experimental data. This research provides a theoretical basis for the design and calculation of group nail connectors in steel–concrete composite structural bridges.

Keywords: Steel–concrete composite structure, Clustered group nail connectors, Bearing capacity reduction, Load-slip relationship

1 Introduction

Shear connectors play a crucial role in steel–concrete composite beams, where they are responsible for transferring longitudinal shear forces between the steel beam and the bridge deck (Wang et al. 2019a; Classen 2018; Yang et al. 2018). The effective combination of steel and concrete is a key factor in ensuring the safe operation of composite structural bridges (Zhang et al. 2023a, 2023b). Among various types of shear connectors, nail connectors are widely used due to their ease of welding and excellent mechanical properties, making them a superior type of flexible shear connector (Wei et al. 2021; Zhang et al. 2018). Particularly in steel truss-concrete composite beams, where the contact surface area between the steel truss's upper chord and concrete is relatively small, it necessitates concentrating multiple nails in a limited area, thus forming clustered group nail connectors (Shi 2021). These group nail locations may be subjected to extreme shear forces, therefore, comprehensive and detailed research on the load-bearing performance

of clustered group nail connectors is especially important. Wuhu Yangtze River Bridge is China's pioneering composite bridge, featuring prestressed concrete bridge panels and steel girders. Embracing the development concept of bridge industrialization and the trend of structural assembly, China has successfully constructed a multitude of prefabricated steel–concrete composite bridges, exemplified by the Hong Kong-Zhuhai-Macao Bridge. Extensive research has demonstrated that densely arranged cluster nailing joints exhibit distinct mechanical properties compared to single nailing. The force distribution among shear nails is non-uniform, resulting in a notable group nailing effect across all stud layers. The average load-carrying capacity of intensive cluster nailing is lower than that of single nailing (Xu et al. 2012). However, the current "Steel Structure Design Standard" (GB50017-2017) (Tong 2019) does not specify any reduction in shear bearing capacity for studs influenced by the group nail effect. Consequently, designing based on the calculation formula for single nails may compromise safety standards. Therefore, it is imperative to conduct a comprehensive study on uneven load transfer between layers of clustered nail joints and establish principles governing reductions in shear bearing capacity. These findings will provide valuable guidance for practical engineering design.

In response to the impact of the group nail effect on bearing capacity reduction, the academic community has proposed various calculation methods. For instance, (Zhou et al. 2014) Zhou et al. analyzed the force characteristics of steel anchor box group nail shear connectors through several finite element models and proposed a formula for the reduction coefficient of shear bearing capacity considering the group nail effect (Deng et al. 2022). Deng et al., through the analysis of 10 push-out specimens and 25 finite element models, found that the load-slip curves of clustered connectors are longer than those of individual nail connectors, with uneven shear forces between the nails and the average shear bearing capacity varying with the spacing and arrangement of nails (Ding et al. 2021). Ding et al. investigated composite nail connectors in Ultra-high performance concrete (UHPC) and found that the nail diameter significantly affects shear performance, while a reduced spacing between nails diminishes performance (Fang et al. 2022). Fang et al. conducted a static analysis of shear connectors in steel-precast UHPC composite structures, explored the impact of nail diameter and plate thickness on shear bearing capacity, and proposed a more accurate strength calculation formula (Zhang et al. 2020). Zhang et al. experimentally investigated the shear resistance of longitudinal double-row nails in self-compacting concrete beams and developed corresponding bearing capacity formulas (Wang et al. 2019b). Although existing research provides quantitative analysis methods for the group nail effect, most national standards, including China's 'Design Code for Steel–Concrete Composite Bridges' (Tong et al. 2020; GB/T 10433–2003), largely do not incorporate the group nail effect in calculations. The reduction coefficients in current standards, mainly based on (Okada et al. 2006) Okada's research, consider only the spacing between nails and the strength of concrete, neglecting the layers of nails along the direction of shear action. This omission could lead to significant errors in estimating the bearing capacity of group nail connectors with multiple layers of nails, impacting practical engineering applications.

Current research commonly employs finite element software to establish numerical models, combined with results from push-out tests, for a comprehensive analysis of the shear bearing capacity and load–displacement behavior of nail connectors. For instance,

Yu et al. (Yu et al. 2020) used a refined three-dimensional nonlinear finite element model to investigate the mechanical behavior of grouped nail shear connectors embedded in hybrid fiber reinforced concrete (HFRC). Shi et al. (Shi and Fan 2022), through finite element model analysis of prefabricated-assembly group nail shear keys, compared the mechanical properties of single and double key groups, thereby deriving a formula for the reduction coefficient of the bearing capacity of multiple key groups. Wang et al. (Wang et al. 2021a) investigated the interaction between nails and UHPC through validation of finite element models and proposed a formula for predicting the shear bearing capacity of nails. Xu et al. (Xu et al. 2022) explored the shear resistance of nail and PBL connectors based on finite element models. Ding et al. (Ding et al. 2017) established detailed finite element models through reverse push-out tests to assess structural shear resistance. Wang et al. (Wang et al. 2021b) used three-dimensional nonlinear finite element models to investigate the multi-bolt effect. However, in the actual engineering design and calculation of steel truss-concrete composite beams, it is necessary to use the load-slip curves of the connectors. Although many standards specify methods for calculating the bearing capacity of nail connectors, they do not provide standard load-slip relationships. Engineers often rely on regression analysis of experimental data or use relationship formulas proposed by other scholars for calculations. For densely arranged clustered group nail connectors, their mechanical properties significantly differ from those of individual nail connectors. When there are multiple layers of nails in the group nail connectors, their initial shear stiffness may experience some reduction. In such cases, using relationship formulas designed for individual nail connectors might overestimate the shear stiffness of group nail connectors, thereby affecting the accuracy of the design.

This paper builds on existing research and uses the finite element simulation method for push-out specimens, comprehensively considering the effects of nail spacing between layers, the number of layers, and concrete strength on the reduction effect of shear bearing capacity. Through regression analysis, a formula for calculating the reduction coefficient of the average bearing capacity of a single nail is derived, and an applicable load-slip relationship expression for clustered group nail connectors is proposed. These achievements not only enrich the theoretical foundation in the field of group nail connectors but also provide an important reference for practical engineering applications.

2 Simulation model

2.1 Finite element model building

2.1.1 Finite element push-out test design

In this paper, we utilized the large-scale spatial finite element software ANSYS 2021 to construct a numerical model of the push-out test. The simulation results were compared with experimental results from other researchers in existing literature to verify the accuracy of the established numerical model. In addition, we conducted a detailed analysis of the force conditions of group nail connectors in the push-out test. The design of the specimens referenced the standard specimen form proposed in the European Code (EC4) (EUROCODE 2004), with adjustments made to the dimensions to accommodate the arrangement of group nails, as shown in Fig. 1.

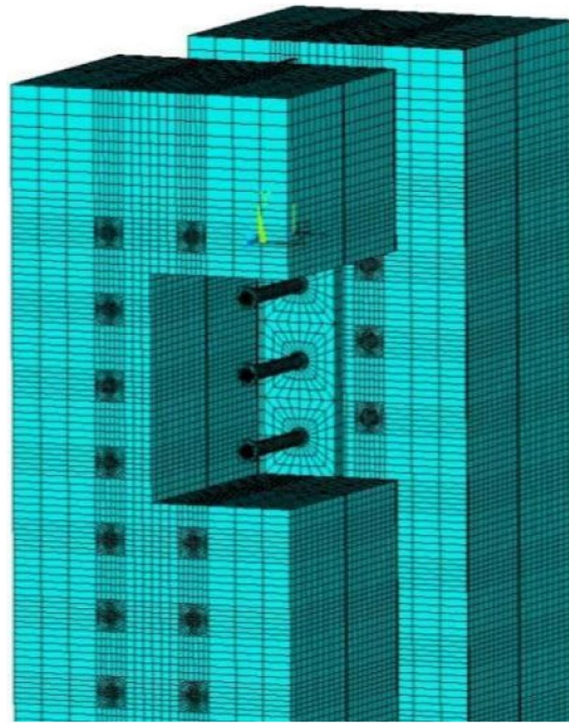


Fig. 2 Mesh generation of finite element model

$\epsilon_u=0.063$, and ultimate strength $f_u=495$ MPa. The Q345 steel has a yield strength $f_y=345$ MPa and an ultimate strength $f_u=480$ MPa. In the finite element model, the constitutive relationship of materials is described using bilinear follow-up strengthening model BKIN and Mises yield criterion with two broken lines having different slopes. The ordinary steel bar used in concrete is HRB335 grade steel bar with ideal elastic–plastic material properties featuring a yield strength $f_y=335$ MPa as shown in Fig. 3.

2.1.3 Simulation of contact relationship between steel and concrete

The model takes into account the friction between the stud and concrete, as well as between the steel beam and concrete. The contact behavior is simulated using the TARGE170 target unit and CONTA175 contact unit, with a friction factor of 0.4. Since the bond between steel and concrete fails at failure time, it is not considered, and the contact gap is closed using element option. In practical engineering, bolts and steel beams are typically connected through welding. In this model, however, the studs and steel beams are treated as a tightly connected entity. When establishing the numerical model, separate mesh models for perforated steel beams and studs are first created respectively. Then, the studs are embedded in predrilled holes of the steel beams while merging repeated nodes to ensure their connection as a whole.

2.1.4 Failure pattern of stud connectors

According to numerous experimental studies and numerical simulation tests, it has been observed that there are two primary failure modes of stud connectors: concrete damage and stud failure.

Table 1 Push-out test models

Concrete	No	Models	Concrete	No	Models	Concrete	No	Models	Concrete	No	Models
C30	1	3R4DC30	C40	26	3R4DC40	C50	51	3R4DC50	C60	76	3R4DC60
	2	3R5DC30		27	3R5DC40		52	3R5DC50		77	3R5DC60
	3	3R6DC30		28	3R6DC40		53	3R6DC50		78	3R6DC60
	4	3R7DC30		29	3R7DC40		54	3R7DC50		79	3R7DC60
	5	3R8DC30		30	3R8DC40		55	3R8DC50		80	3R8DC60
	6	4R4DC30		31	4R4DC40		56	4R4DC50		81	4R4DC60
	7	4R5DC30		32	4R5DC40		57	4R5DC50		82	4R5DC60
	8	4R6DC30		33	4R6DC40		58	4R6DC50		83	4R6DC60
	9	4R7DC30		34	4R7DC40		59	4R7DC50		84	4R7DC60
	10	4R8DC30		35	4R8DC40		60	4R8DC50		85	4R8DC60
	11	5R4DC30		36	5R4DC40		61	5R4DC50		86	5R4DC60
	12	5R5DC30		37	5R5DC40		62	5R5DC50		87	5R5DC60
	13	5R6DC30		38	5R6DC40		63	5R6DC50		88	5R6DC60
	14	5R7DC30		39	5R7DC40		64	5R7DC50		89	5R7DC60
	15	5R8DC30		40	5R8DC40		65	5R8DC50		90	5R8DC60
	16	6R4DC30		41	6R4DC40		66	6R4DC50		91	6R4DC60
	17	6R5DC30		42	6R5DC40		67	6R5DC50		92	6R5DC60
	18	6R6DC30		43	6R6DC40		68	6R6DC50		93	6R6DC60
	19	6R7DC30		44	6R7DC40		69	6R7DC50		94	6R7DC60
	20	6R8DC30		45	6R8DC40		70	6R8DC50		95	6R8DC60
	21	7R4DC30		46	7R4DC40		71	7R4DC50		96	7R4DC60
	22	7R5DC30		47	7R5DC40		72	7R5DC50		97	7R5DC60
	23	7R6DC30		48	7R6DC40		73	7R6DC50		98	7R6DC60
	24	7R7DC30		49	7R7DC40		74	7R7DC50		99	7R7DC60
	25	7R8DC30		50	7R8DC40		75	7R8DC50		100	7R8DC60

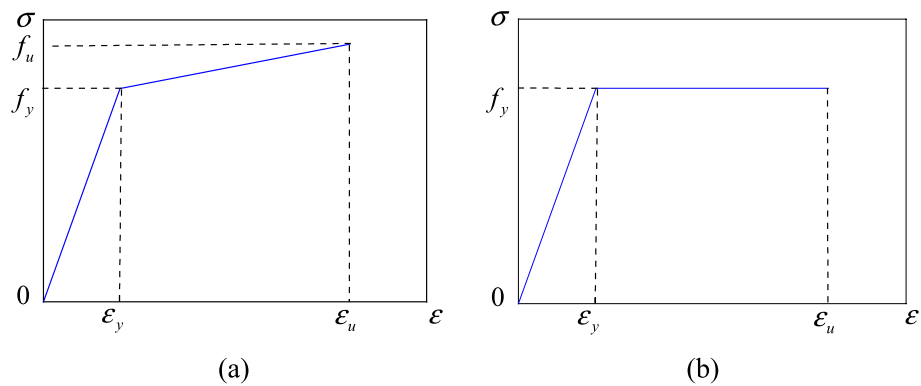


Fig. 3 Selection of constitutive relation of steel (a) Constitutive relationship of ML15 and Q345 steels (b) Constitutive relation of ordinary reinforcement

The failure of concrete typically occurs when its strength is relatively weaker compared to the material strength of the stud. Concrete failure mainly manifests in two forms: compression failure and splitting failure. During the push-out test, significant compressive stress is exerted by the stud on the concrete in front of the loading direction. This stress primarily concentrates near the root of the stud, eventually leading to localized crushing or splitting of concrete in that region. Shear failure is commonly encountered

as a mode of stud failure. When the material strength of the stud is comparatively lower than that of concrete, shear failures occur due to substantial shear forces acting on the root area of studs. Additionally, other types of damage may also arise including weld damage, steel beam base metal damage, and bolt pulling out damage; these should be avoided during design and construction processes. Poor welding quality can result in premature fracture at welds before reaching material strength while good welding quality leads to shear failures within studs themselves. Increasing length-to-diameter ratio for studs can help prevent pullout damages.

2.2 Finite element analysis model verification

2.2.1 Shear bearing capacity and load-slip curve

The results obtained by the finite element model will be verified in this section. The parameters and test sources of the selected specimens are presented in reference (Luo 2008; Li 2015; Zhang 2021; Lin and Liu 2015). The numerical model was established based on the modeling method described in Sect. 2.1 of this paper. The material size and parameters of the model were all referenced from Table 1, while the load-slip curve of the specimen was extracted and compared with test data from reference (Huang 2015; Xu 2013) for validation purposes. The corresponding results are presented in Fig. 4.

As can be seen from Fig. 4, the load-slip curve obtained by the numerical simulation test in this paper is in good agreement with the test results, and there is no significant deviation in the curve during the loading process, which indicates that the numerical simulation model established in this paper can accurately simulate the test process of connector ejection.

3 The force mechanism of clustered group nail connectors

3.1 The group nail effect of clustered group nail connectors

Clustered group nail connectors exhibit significant differences in mechanical performance compared to traditional connectors with uniformly distributed individual nails, mainly due to the so-called 'group nail effect'. During the loading process, the distribution of loads among the nails in different layers of group nail connectors is uneven. This results in a reduction in both shear stiffness and shear-bearing capacity compared to

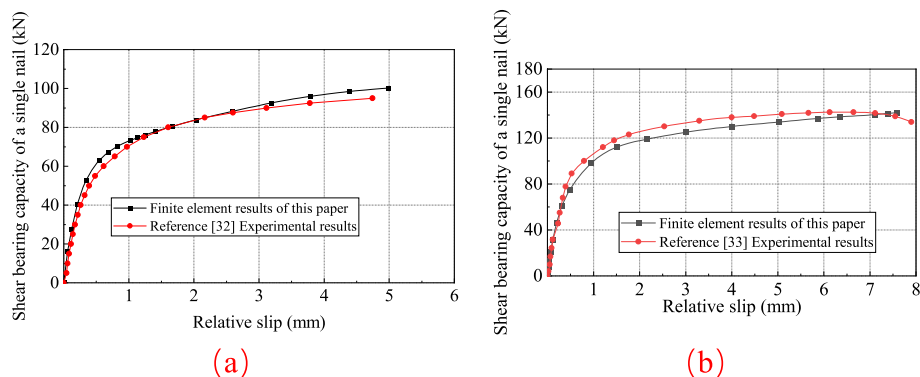


Fig. 4 Comparison of finite element model and experimental load-slip curve

single-row nail connectors. Particularly in the failure stage, group nail connectors may exhibit a cascading failure effect similar to 'falling dominoes' (Lian 2015).

3.1.1 Load-slip relationship under group nailing effect

Figure 5 presents the load-slip curves of push-out specimen models with different numbers of nail layers, based on specific model parameters (nail diameter 22 mm, nail height 200 mm, layer spacing 5D, i.e., five times the nail diameter). This curve clearly reveals the two main stages in the loading process of the nail connectors: the elastic stage and the elasto-plastic stage. In the initial phase of loading, the curve exhibits a linear trend, indicating small slip amounts and suggesting that the material of the connector is in the elastic state. As the loading continues, the connector gradually enters the elasto-plastic stage. The rate of increase in slip amount accelerates, and although the connector has not yet reached the yield point, it already exhibits certain ductile characteristics.

3.1.2 Reduction of load bearing capacity of group nail connectors

By synthesizing experimental data from multiple scholars (Deng et al. 2022; Su et al. 2014), we have compiled information on the average shear bearing capacity and shear stiffness of individual nails in Table 2, and conducted a comparative analysis with clustered group nail connectors. It is observed that the average bearing capacity of individual nails in clustered group nail connectors significantly decreases compared to individual nail connectors, and this decrease is positively correlated with the number of nail layers. Specifically, as the number of nail layers increases, the reduction in the average shear bearing capacity of individual nails gradually intensifies. Similarly, the shear stiffness of group nail connectors also decreases with an increase in the number of nail layers.

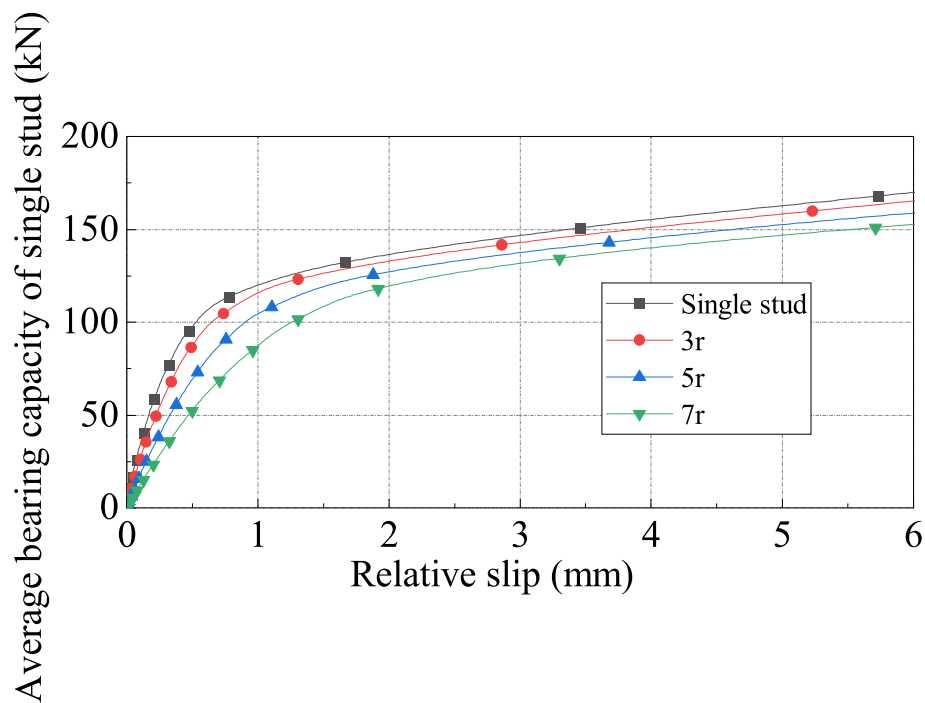


Fig. 5 Load-slip curve of cluster nail connectors with different numbers of nail layers

Table 2 Load-bearing capacity and shear stiffness reduction of cluster nail connectors

No	shear stiffness (kN/mm) K_s	reduction factor η	Average shear bearing capacity(kN) P_s	reduction factor η
Single nail	170.99	1	169.9	1
3R5DC50	142.22	0.832	163.8	0.964
4R5DC50	127.04	0.743	160.0	0.942
5R5DC50	106.90	0.625	157.1	0.924
6R5DC50	99.51	0.582	152.9	0.901
7R5DC50	87.76	0.513	148.2	0.871

3.1.3 Mechanical characteristics of group nail connectors

In the experiment, the loading point is located at the top of the steel beam, and the vertical force F is applied to the top of the steel beam, causing shear forces at the base of the nails in the concrete. This shear force is transmitted to the concrete in the form of a vertical force. The lower end of the concrete is constrained, and under the action of shear force in the nails and the bonding force with the steel beam, it undergoes certain compressive deformation. Since the bottom end of the steel beam is not constrained, there is no vertical compression deformation, causing the distances between the welding points of each layer of nails and the distances between the nail heads to be unequal. This results in a certain 'arch-shaped' deformation of the steel plate, where the deformation of the steel plate leads to the nails bearing a portion of additional force, resulting in a decrease in shear force in the upper nails and an increase in shear force in the lower nails, as shown in Fig. 6.

Using ANSYS 2020, the shear forces borne by each layer of nails in each loading stage are calculated. Taking the example of a 7-layer clustered group nail connector with a

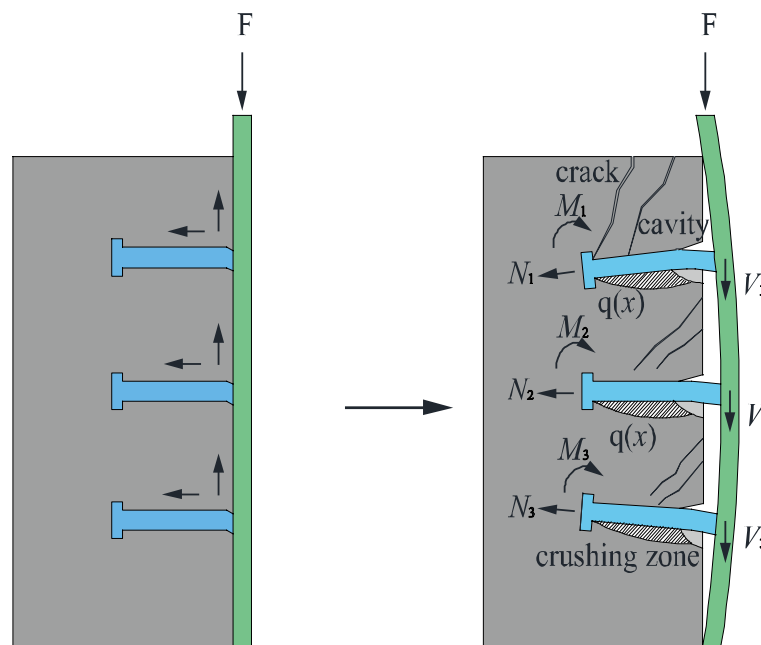


Fig. 6 "Arch" deformation of push-out specimen

diameter of 19 mm and a height of 200 mm, by selecting all the nodes at the bottom of the nails in the solid model and calculating the sum of the forces in the y-direction, the shear force value borne by each nail is obtained. Figure 7 shows the load values borne by each row of nails at different stages. It can be noted that from top to bottom, the shear force values borne by the nails first decrease and then increase, exhibiting a 'saddle-shaped' distribution. The bottom layer of nails bears the maximum shear force, which is consistent with the analytical results of the 'arch-shaped deformation' theory. Therefore, the bottom layer of nails is the first to shear during failure.

Furthermore, in the initial loading stage, the uneven distribution of forces among the nails in each layer is high, but as the load increases, the forces among the nails in each layer tend to become more uniform. For example, at a load of $0.2P$, the sum of the shear forces borne by the first, sixth, and seventh layers of nails compared to the sum of the shear forces borne by all layers of nails shows that 42% of the nails bear 48% of the overall shear force, indicating a relatively uneven force distribution."

The unevenness coefficient is introduced to quantitatively describe the unevenness of the forces on each layer of nails in the clustered group nail connector. This paper adopts the method from reference (Li 2017), leveraging the calculation principle of the Gini coefficient G , to define a method suitable for calculating the unevenness of the forces on each layer of nails. The arrangement of each layer of stud in ascending order according to the load borne is illustrated in Fig. 8. The horizontal axis represents the cumulative proportion of the number of stud layers, while the vertical axis represents the cumulative load proportion corresponding to the cumulative number of layers, with each point being connected. η denotes the ratio between the area of part B and the sum of areas for parts A and B in the Fig. 8.

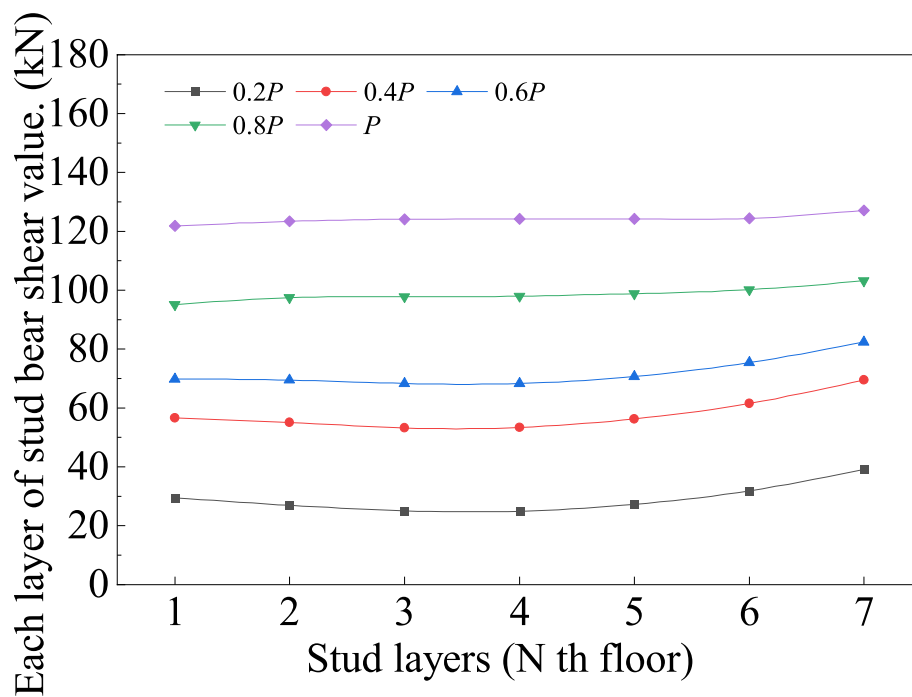


Fig. 7 Shear distribution of nails in different layers under different loads

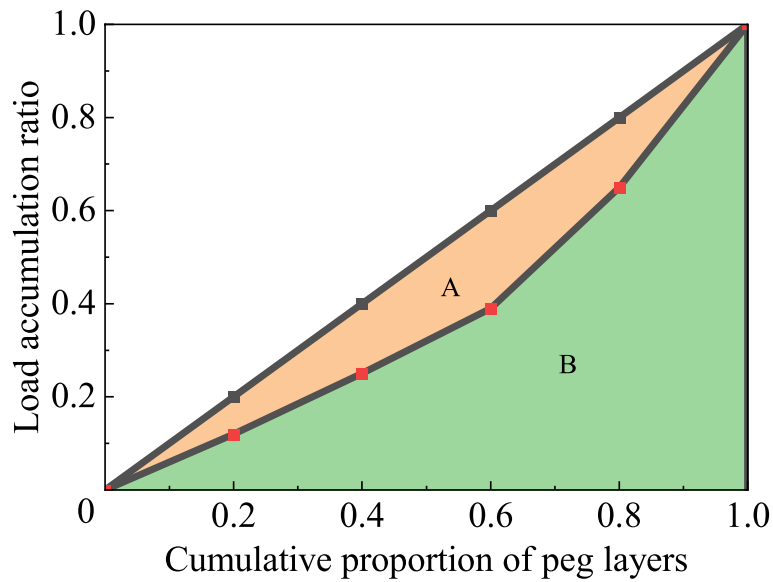


Fig. 8 Influencing factors of non-uniformity coefficient. **a** The impact of nail layer spacing on the unevenness coefficient. **b** The influence of concrete strength on the unevenness coefficient

$$\eta = \frac{S_B}{S_A + S_B} \tag{1}$$

The unevenness coefficient for the clustered group nail connector is calculated at five load levels. Taking examples of 5R-6D-C50, 5R-8D-C50, as well as 7R-5D-C40, and 7R-5D-C50, the variation curves are plotted, as shown in Fig. 9. In the stages before $0.6P$, due to the delayed transmission of the load, the nails at the loading end bear a larger load, and the distribution of forces on the nails along the shear direction shows a 'saddle-shaped' pattern. When the load reaches $0.8P$, as the volume of the material in the plastic stage continues to increase, the stress redistribution effect becomes more pronounced. At this point, the forces on each layer of nails are generally uniform, with the layer experiencing the maximum force located on the side away from the loading end.

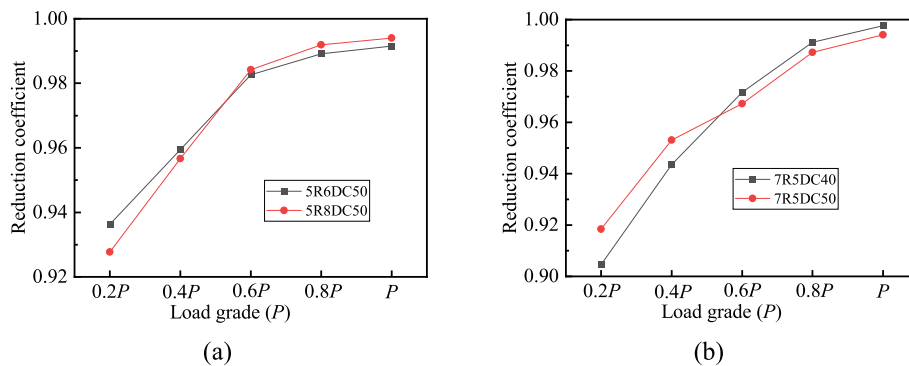


Fig. 9 Calculation diagram of uneven force coefficient of stud

3.2 The force transmission mechanism of clustered group nail connectors

3.2.1 Load-slip relationship under group nailing effect

During the loading process of the specimen, the concrete region near the base of the bolts experiences high triaxial compressive stress. Shear, bending moment, and eccentric normal forces reach equilibrium at a certain distance from the steel–concrete interface. Taking a 22 mm diameter, 5D spacing, and 7-layer clustered group nail connector as an example, Fig. 10(a) shows the front view of the principal stress cloud. The gray area indicates the concrete reaching the limit of principal compressive stress in that region and being crushed. As the load increases, the load is gradually transmitted from the top layer of bolts to the bottom layer of bolts. Due to the restraint at the bottom of the concrete, the gray stress area of the bottom layer of bolts increases accordingly. Figure 10(b) is the profile principal stress cloud map of the concrete-bolt axis. The contour lines of vertical stress on the bolt form a triangle, with a larger high-stress area near the base of the bolt, and the stress values gradually decrease away from the bolt base. The area of the crushed zone also shows a similar changing pattern. Overall, the crushed zone on the profile map appears as a triangle that gradually increases with the increasing load.

3.2.2 The stress state of the nails

Taking the example of a 7-layer bundled nail connection with a nail diameter of 22 mm and a nail layer spacing of 5D, the failure test was conducted. From Fig. 11, it can be observed that the maximum shear stress occurs at a position approximately 10 mm from the nail root, with a value of up to 271 MPa. Beyond this position, the shear stress rapidly decreases. Simultaneously, the maximum axial stress occurs near the nail root. The critical section for nail failure is within approximately 10 mm from the root, where failure typically occurs. At a distance of around 50 mm from the nail root, the stress direction changes, reaching another extreme point. This is due to the application of downward vertical force at this stage, and the concrete beneath the nail has already been crushed, lacking effective restraint. The stress state at this point is similar to that of a cantilever beam with one end fixed and the other end subjected to a concentrated downward force, causing compression on the lower side and tension on the upper side of the nail.

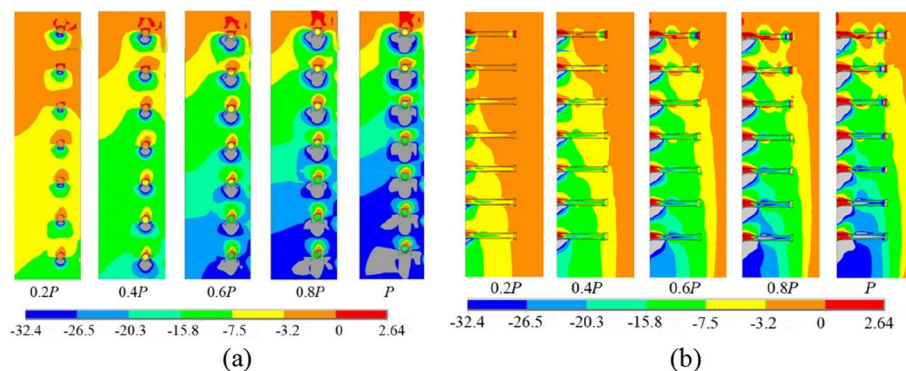


Fig. 10 Nephogram of principal compressive stress in normal and profile of concrete (Unit: MPa). **a** Nephogram of principal compressive stress in normal concrete. **b** Nephogram of principal compressive stress in profile of concrete

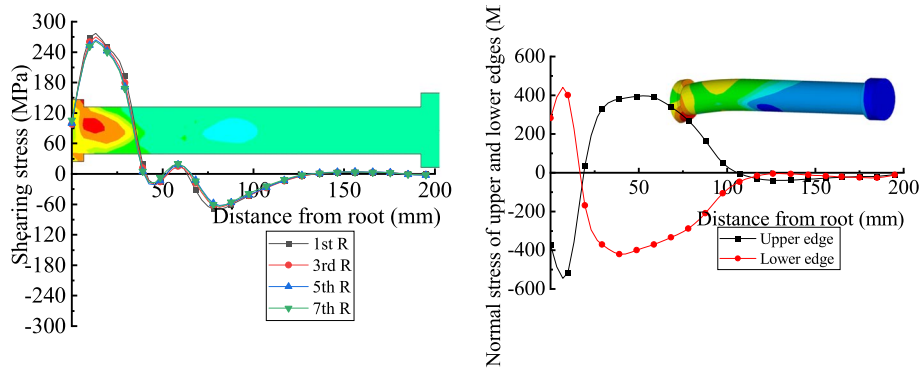


Fig. 11 Diagram of axial distribution of shear stress and axial stress of nail

4 Parametric analysis of clustered group connections

4.1 Layer arrangement of clustered group connections

Using a bolt diameter of 19 mm as an example, Fig. 12 compares the average shear force of a single bolt under different bolt layer numbers. The increase in bolt layers results in a decrease in the average load-carrying capacity of a single bolt, and the corresponding reduction coefficient also decreases. When the nail layers increase from 3 to 7R, the reduction ratio increases from 3.6% to 13.5%. Therefore, the influence of nail layers cannot be ignored. Figure 13 shows the variation of the unevenness coefficient for connectors with different numbers of layers. The increase in nail layers leads to a decrease in the unevenness coefficient, indicating a more pronounced uneven force distribution. With the increase in load value, the unevenness coefficient becomes larger, suggesting a tendency towards uniform loading. When the load reaches its limit, the force distribution becomes relatively uniform.

According to the provisions of the European standard (EC4) regarding shear stiffness, which is the ratio of the shear carrying capacity multiplied by 0.9 times the safety factor

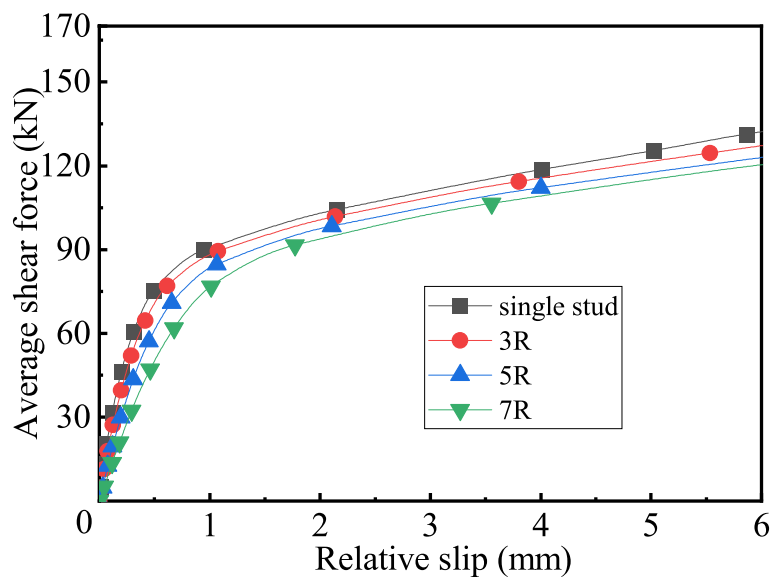


Fig. 12 Influence of number of nail layers on load-slip curve

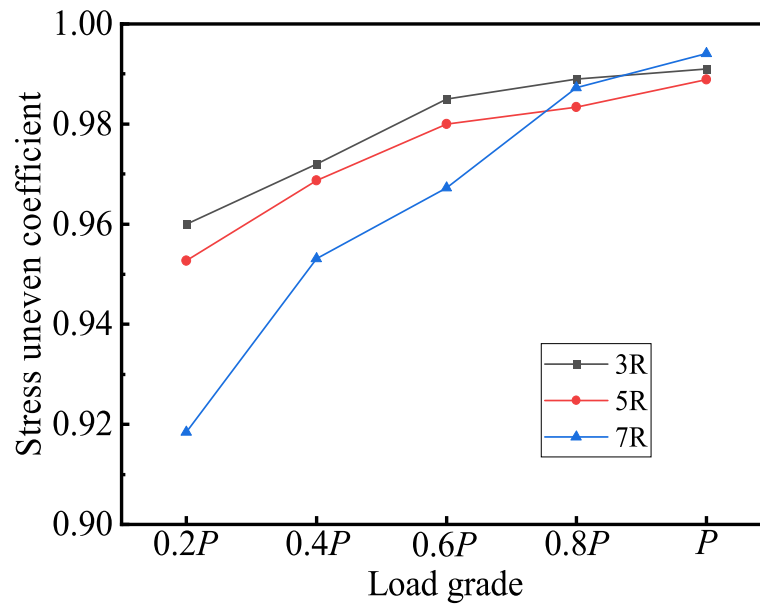


Fig. 13 Variation of uneven coefficient of stress on connectors with different layers

to 0.7 times the slip value, Fig. 12 reveals that the increase in nail layers has a significant impact on shear stiffness. Combining the above conclusions, it is evident that a few nails bear the majority of the load, leading to an overall reduction in the stiffness of bundled nail connections. Due to the premature yielding of the nail root, which bears a significant shear force in the initial stage, and subsequent internal force redistribution, the force gradually becomes more uniform, making this phenomenon particularly pronounced in the initial stage.

Table 3 quantifies the ratio of uneven force distribution to shear stiffness, using the tangent stiffness at $0.9 \times 0.7P$, primarily reflecting the average stiffness in the initial stage. It can be concluded that the higher the uneven force distribution, the smaller the shear stiffness. Therefore, the average shear capacity of bundled bolt connections is lower than that of single-bolt connections in the initial loading stage.

4.2 Spacing of clustered group connections

Taking $d=22$ mm, a fixed number of layers as 5 layers, and C50 concrete as an example, the influence of different bolt spacings on shear bearing capacity and uneven force distribution is analyzed. Figures 14 and 15 provide a comparison of the load-slip curves and unevenness coefficients for different bolt spacings, while Table 3 presents the variation of reduction coefficients. From Fig. 14 and Table 4,

Table 3 Influence of the number of nail layers on shear stiffness

Types of models	Single nail	3R	5R	7R
Shear stiffness (kN/mm)	163.33	142.22	106.90	81.42
Stiffne reduction factor	1	0.871	0.654	0.499
Uneven coefficient λ at 0.2P	1	0.96	0.95	0.918
Uneven coefficient λ at 0.4P	1	0.972	0.969	0.953

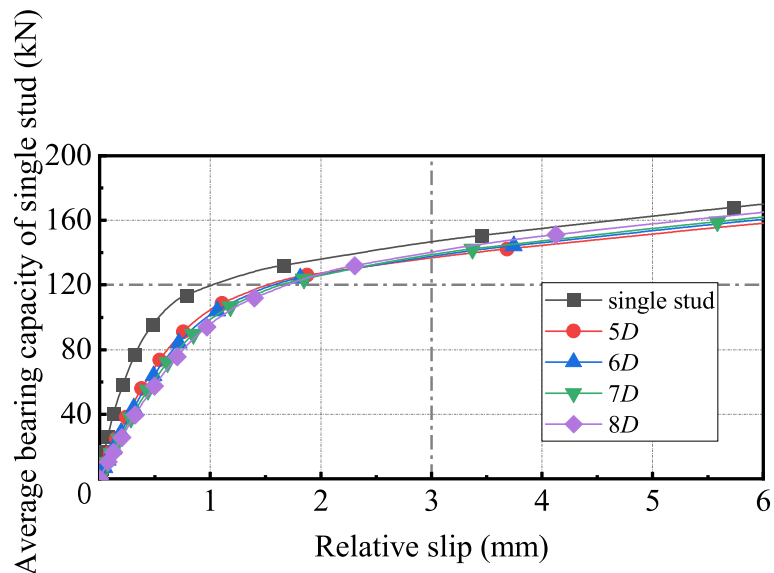


Fig. 14 Load-slip curves under different nail spacing

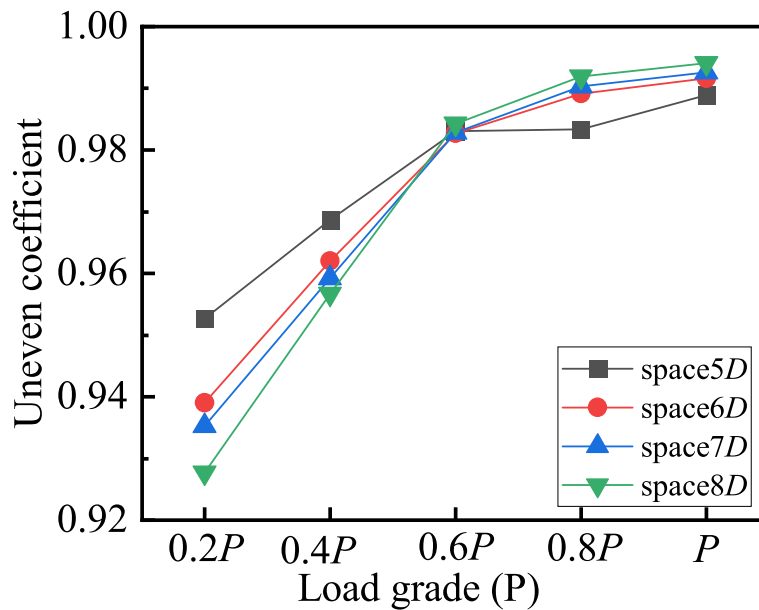


Fig. 15 Influence of spacing between nail layers on non-uniformity coefficient

Table 4 Influence of nail spacing on bearing capacity

Types of models	Nail diameterd = 22 mm					
	Single nail	4D	5D	6D	7D	8D
Average bearing capacity of single nail (kN)	169.9	156.31	156.99	159.03	160.90	162.93
Reduction factor η	1	0.920	0.924	0.936	0.947	0.959

it can be observed that a too-small bolt spacing will decrease the average bearing capacity of a single bolt. When the bolt spacing is reduced from 8 to 4d, the bearing capacity of a single bolt decreases by 4%. Figure 15 shows a significant variation in the unevenness coefficient before $0.6P$, and a larger spacing results in a more uneven force distribution. As the load approaches the limit, the force gradually becomes more uniform.

Table 5 illustrates the impact of bolt spacing on shear stiffness. It can be seen that shear stiffness is positively correlated with uneven force distribution. The initial uneven force distribution causes more load to be distributed to a few bolts, leading to a reduction in the average shear stiffness of the bundled bolt connection in the initial stage.

4.3 Influence of concrete strength grade

Figure 16 illustrates the variation in load-slip curves for different concrete strength grades. It can be observed that the concrete strength grade is negatively correlated with the reduction coefficient; the higher the concrete grade, the lower the corresponding reduction. Taking $d=22$ mm, a bolt spacing of 4D, and a 3-layer bundled bolt connection as an example, when the concrete grade increases from C30 to C60, the reduction coefficient decreases from 10.7% to 3.8%. With an 8D bolt spacing, using C30 concrete results in only a 1.3% reduction compared to C60. This implies that in engineering, not only can the utilization of bolts be improved by using high-strength concrete, but a part of the reduction in stiffness due to lower concrete strength can also be compensated for when the bolt spacing is larger.

Table 5 Influence of nail spacing on shear stiffness

Types of models	Single nail	5D	6D	7D	8D
Shear stiffness (kN/mm)	163.33	106.90	100.50	94.87	89.85
Reduction factor η	1	0.654	0.615	0.581	0.550
Uneven coefficient λ at $0.2P$	1	0.953	0.939	0.935	0.928

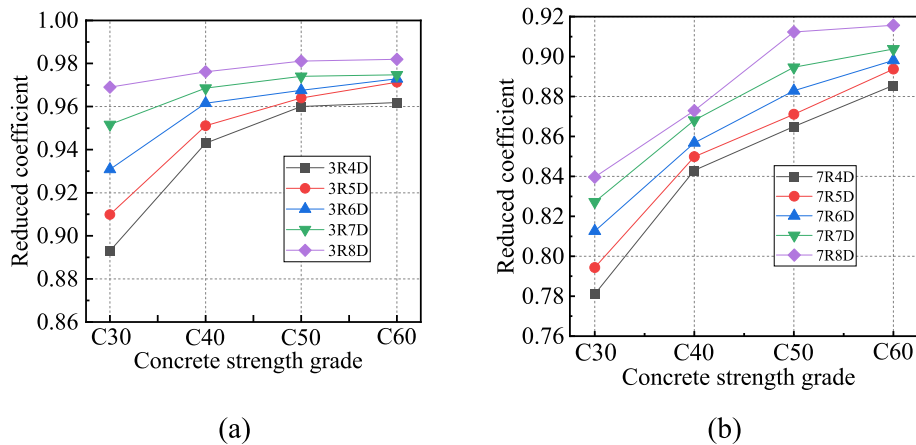


Fig. 16 Load-slip curves under different concrete strength grades. **a** 3 layer group nail connectors. **b** 7 layer group nail connectors

Figure 17 shows the influence of concrete strength grades on the uneven force distribution coefficient. It can be seen that before 0.6P, the impact of concrete grades on uneven force distribution is significant, but becomes negligible when approaching the limit. In Fig. 18, taking a 5-layer bundled bolt connection with an 8D bolt spacing as an example, at the ultimate bearing capacity, the principal stress cloud diagram under each concrete strength grade reveals that the crushing area for the connection using C30 concrete is 50.72% larger than that using C60 concrete. Using higher strength concrete effectively reduces the crushing area, avoiding complete crushing before the bolt shearing occurs. In

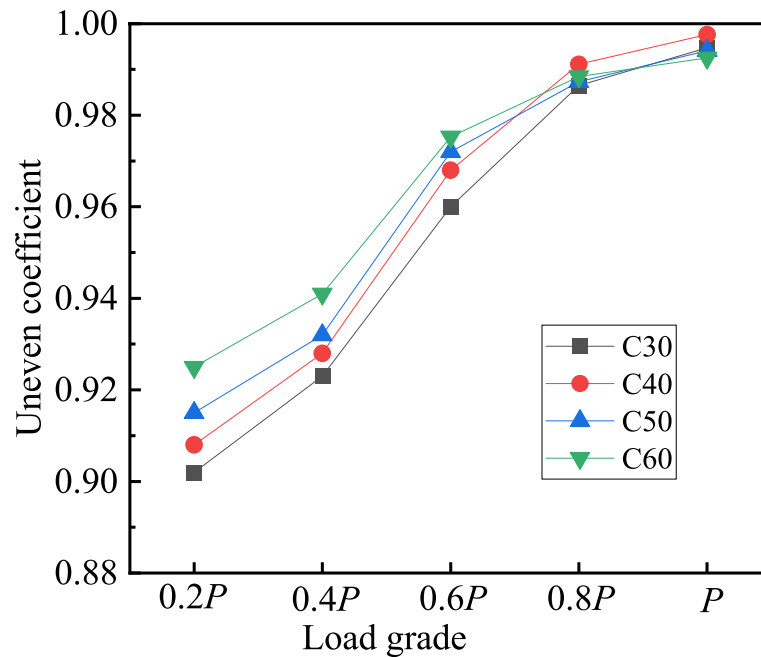


Fig. 17 Influence of concrete strength grade on uneven coefficient

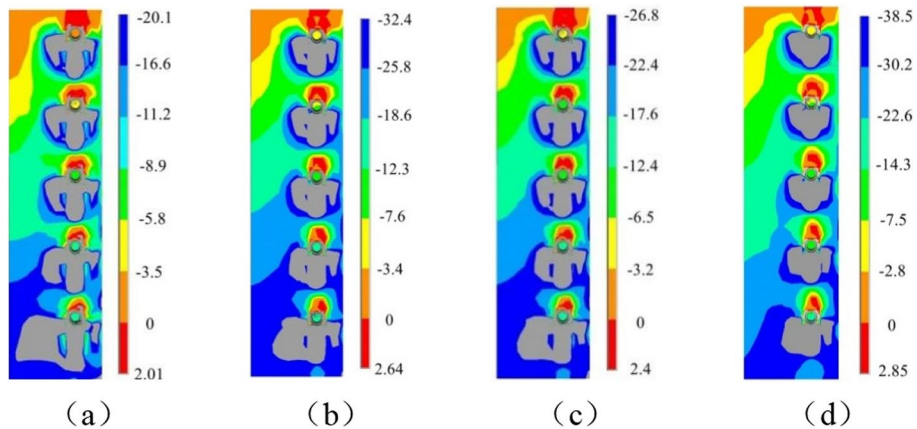


Fig. 18 Influence of concrete strength grade on principal compressive stress of concrete with group nail connector. **a** principal compressive stress of C30. **b** principal compressive stress of C40. **c** principal compressive stress of C50. **d** principal compressive stress of C60

summary, increasing the concrete strength grade helps reduce the main stress in concrete, decrease the crushing area, and enhance the bearing capacity of bundled bolt connections.

5 Calculation methods for bearing capacity and slip of connections

5.1 Reduction coefficient calculation

The calculation of the reduction coefficient for the group bolt effect, considering the coupling effects of bolt spacing and bolt layers at multiple levels, based on concrete strength classification, yields the shear capacity reduction coefficient. Figure 19 presents a three-dimensional surface, where the Z-axis represents the shear capacity reduction coefficient, and the X and Y axes represent the bolt layers and bolt spacing, respectively, with concrete strength as a fixed parameter. The three factors listed have a significant impact on the reduction coefficient values. As the concrete strength grade increases, the surface is positioned higher in the coordinate system, emphasizing the importance of considering concrete strength as an influencing factor.

This paper conducted a multivariate regression analysis using MATLAB 2020 software to fit a formula incorporating the three factors mentioned above. Here is the definition of this formula:

$$y = a_1x_1 + a_2x_1^2 + a_3x_2 + a_4x_2^2 + a_5x_3 + a_6x_3^2 + a_7 \tag{2}$$

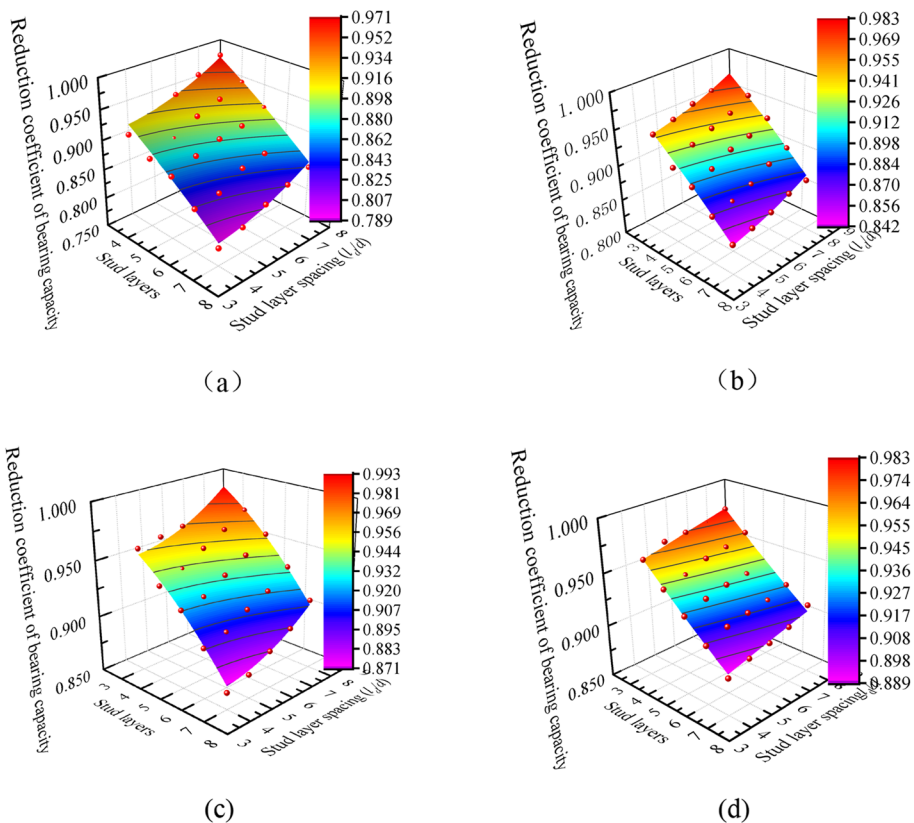


Fig. 19 Fitting surface with reduction coefficient under multifactor coupling. **a** Concrete strength C30. **b** Concrete strength C40. **c** Concrete strength C50. **d** Concrete strength C60

In Eq. (2), x_1, x_2, x_3 and serve as the three independent variables, y is the dependent variable, and a_1, a_2 are unknown parameters.

The results obtained from the least squares fitting are as follows:

$a_1 = -0.0076, a_2 = 0.0088, a_3 = 0.0090, a_4 = -0.0016, a_5 = 0.0001, a_6 = -0.0001, a_7 = 0.7020$, The residual value is 0.0085, and the error is within an acceptable range. Substituting the calculated results into Eq. (2) and simplifying, the obtained results are as follows:

$$y = a_1x_1 + a_2x_2 + a_3x_3 + a_4x_1^2 + a_5x_3^2 + a_6 \quad (3)$$

In Eq. (3), it was observed that the influence of the independent variable on the result can be negligibly small. Therefore, removing this term still yields a good fit. The coefficients obtained from the re-fitted least squares method are:

$$a_1 = -0.0076, a_2 = 0.01, a_3 = 0.0090, a_4 = -0.0016, a_5 = -0.0001, a_6 = 0.6985,$$

Substituting the calculated coefficients into Eq. (3), we obtain:

$$y = \left(-76x_1 + 100x_2 + 90x_3 - 16x_1^2 - x_3^2 \right) \times 10^{-4} + 0.6985 \quad (4)$$

The independent variables x_1, x_2 and x_3 are respectively brought into the number of bolt layers n_r , the spacing of the layer of the bolt n_d , and the compressive strength $f_{cu,k}$ of the concrete cube, respectively, to obtain the formula of the reduction coefficient of the shear bearing capacity of the cluster group nail:

$$\eta = \left(-76n_r + 100n_d + 90f_{cu,k} - 16n_r^2 - f_{cu,k}^2 \right) \times 10^{-4} + 0.6985 \quad (5)$$

5.2 Calculation methods for shear bearing capacity and slip of clustered connection

The original load-slip curve proposed for single-nail connectors has a certain deviation when applied to the cluster group nail connectors, which will overestimate the shear stiffness in the initial stage of loading. Therefore, this section intends to refit a load-slip relationship suitable for cluster group nail connectors based on the existing research results in this paper and the load-slip curve data of various types of cluster group nail connectors. It is pointed out that the number of nail layers and the spacing of the nail layers will affect the initial shear stiffness of the cluster group nail connector, and the influence of the number of nail layers n_r and the spacing of the nail layer n_d on the load-slip curve will be considered in this section.

Taking the concrete strength of C50 as an example, combined with the load-slip curve data obtained by the number of bolt layers and the spacing of bolt layers, the calculation is carried out for many times, and it is considered that the fractional form of the Buttry formula is simple and the fitting effect is good, so the proposed formula form is as follows:

$$Q = \frac{bS}{1 + aS} \quad (6)$$

Given the initial values $a = 1$ and $b = 1$, 12 sets of typical data are substituted into (6), and the least squares method is used to fit and iterate repeatedly, and the following data are finally obtained, as shown in Table 6:

Table 6 Fitting value of formula coefficient

	3R5DC50	5R5DC50	7R5DC50	3R6DC50	5R6DC50	7R6DC50
<i>b</i>	1.95689	1.38823	1.0096	1.77517	1.24431	0.89903
<i>a</i>	1.85343	1.22017	0.8260	1.61997	1.06921	0.71535
<i>b-a</i>	0.10346	0.16806	0.1836	0.1552	0.1751	0.18368
	3R7DC50	5R7DC50	7R7DC50	3R8DC50	5R8DC50	7R8DC50
<i>b</i>	1.68823	1.15505	0.8111	1.60598	1.05619	0.67428
<i>a</i>	1.55352	0.99049	0.6294	1.46321	0.88131	0.51468
<i>b-a</i>	0.13471	0.16456	0.1817	0.14277	0.17488	0.1596

a is taken as the dependent variable, and the number of nail layers and the spacing of the nail layers are taken as independent variables, and the relationship is determined after trial calculation:

$$a = a_1 - a_2 n_r + \frac{a_3}{n_r} - a_4 n_d + \frac{a_5}{n_d} \quad (7)$$

If $a_1 = 1$, $a_2 = -0.11123$, $a_3 = 2.666$, $a_4 = -0.051$, $a_5 = 2.5$, then *a* is denoted as:

$$a = 1 - 0.11123 n_r + \frac{2.666}{n_r} - 0.051 n_d + \frac{2.5}{n_d} \quad (8)$$

Then *b* is determined by *b-a*, and through the linear relationship of n_r , the following is proposed:

$$\Delta = b - a = 0.09561 + 0.01351 n_r \quad (9)$$

In summary, it can be obtained that the load-slip full curve relationship of the cluster group nail connector:

$$Q = Q_u \frac{bS}{1 + aS} \quad (10)$$

$$a = 1 - 0.11123 n_r + \frac{2.666}{n_r} - 0.051 n_d + \frac{2.5}{n_d} \quad (11)$$

$$b = a + \Delta = 0.09561 + 0.01351 n_r \quad (12)$$

Which is also suitable for 3~7 layers of bolts, 4d~8d bolt layer spacing and C30~C60 concrete. where: *S* represents the amount of slip in mm; *Q* represents the shear force of the nail in kN; Q_u is the design value of the shear bearing capacity of the nail, and the unit is kN; n_r represents the number of bolt layers of cluster group nail connectors; n_d represents the relative layer spacing of the nails, i.e., $n_d = \frac{l_d}{d}$, in mm.

This formula is applicable to the range of $3 \leq n_r \leq 7$, $4 \leq n_d \leq 8$, concrete strength C30~C60.

5.3 Verification

The data from reference (Deng et al. 2022) was used for validation with parameters as shown in Table 7. A selection was made for 3 layers and C50 concrete with 4d to 8d spacing for the connection. Figure 20 presents a comparative graph between experimental data from Table 6 and calculated results using the proposed formula. The load-slip relationship curves, obtained by the formula provided in this paper, align well with the experimental data, showing minimal deviation. Table 8 provides the shear stiffness results for each test group along with their corresponding curves. Due to accidental factors, the data of GS2 specimen is significantly higher than that of other specimens. It can be observed that, except for GS2, the errors are within 10% for the other three groups, with a mean value of 8.22%.

Table 7 Parameters of push-out specimen used to verify formula

No	Data source	Nail size (diameter mm × height) (mm)	Nail layers	Nail layers spacing (D)	Concrete strength grade
GS1	Deng (Deng et al. 2022)	16 × 150	3	4D	C50
GS2	Deng (Deng et al. 2022)	16 × 150	3	6D	C50
GS3	Deng (Deng et al. 2022)	16 × 150	3	8D	C50
GS4	Deng (Deng et al. 2022)	16 × 150	5	4D	C50

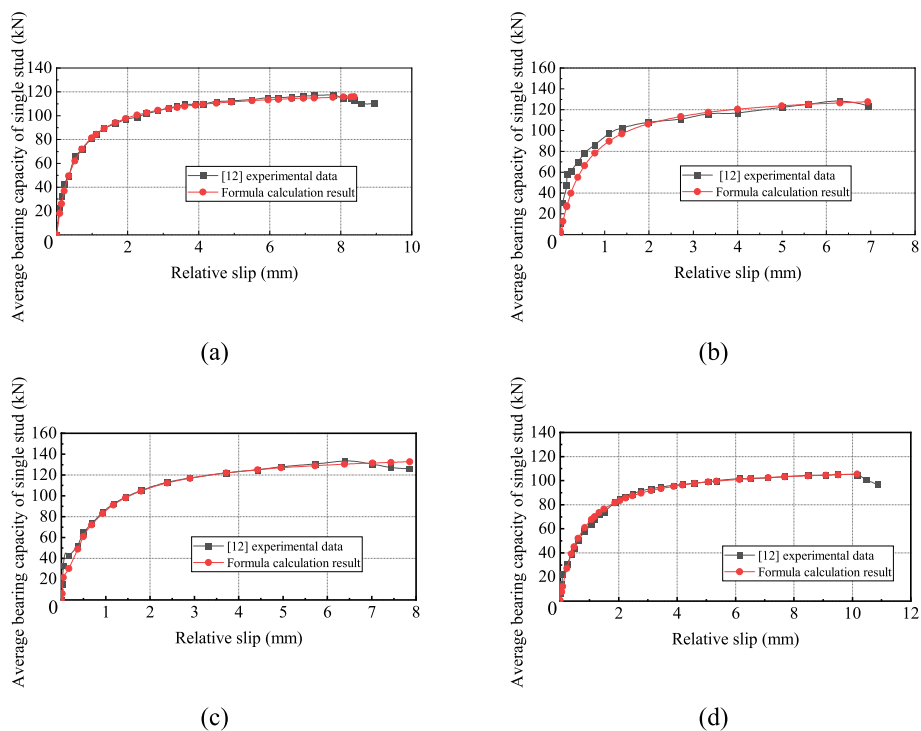


Fig. 20 Verification result of curve formula. **a** Verification result of GS1. **b** Verification result of GS2. **c** Verification result of GS3. **d** Verification result of GS4

Table 8 Comparison of shear stiffness (Unit: kN/mm)

No	Test result	Formula calculation result	calculation error
GS1	95.36	98.76	3.57%
GS2	124.76	101.52	18.63%
GS3	90.43	88.2	2.47%
GS4	59.25	64.10	8.19%

6 Conclusions

- (1) The phenomenon of group effect significantly impacts the load-carrying capacity and shear stiffness of individual bolts within bundled connections. For bolt numbers ranging from 3 to 7 in rows and 4 to 8 in columns, and with concrete strengths varying between C30 and C60, the ultimate load capacity's reduction coefficient spans from 0.781 to 0.982. This effect leads to a decrease in connection shear stiffness by as much as 50%. It is imperative for design considerations to adequately address the diminished bolt shear capacity and stiffness due to the group effect.
- (2) The root cause of the group effect lies in the uneven force distribution among bolts positioned on different layers. The load is transmitted in a stepwise manner, initially placing a greater shear force on the upper bolts because of the sequence of load transmission. The constraints imposed by the concrete's bottom surface significantly restrict bolt displacement, culminating in increased shear forces on both upper and lower bolts, while intermediate bolts experience lower forces. This uneven distribution is particularly noticeable at the onset of loading but becomes more uniform as the load intensifies, eventually leading to plastic deformation in both steel and concrete.
- (3) The decrease in average load-carrying capacity for bolts in bundled connections exhibits a direct positive correlation with the number of bolt layers and a negative correlation with both bolt spacing and concrete strength. Similarly, the force distribution's unevenness and the reduction in shear stiffness within bundled connections are positively correlated with the number of bolt layers and spacing, and inversely correlated with concrete strength. Among these factors, bolt layers exert the most significant influence on the reduction of load capacity, with bolt spacing and concrete strength playing comparable roles.
- (4) Numerical simulations have yielded 100 sets of coefficients pertinent to the reduction in bundled connection capacities, facilitating the establishment of a comprehensive load-slip expression tailored for bundled connections. The derived shear stiffness curve demonstrates an average deviation of 8.22% from experimental values, underscoring the simulation's accuracy.
- (5) Despite delving into the mechanics of forces and group effects in bundled connections, there remains a clear need for further research. Specifically, more detailed investigations are required to quantify the group effect in the context of new concrete materials and to develop a refined slip relationship.

Authors' contributions

Methodology, S.W. and C.T.; validation, S.W., G.L. and Y.F.; formal analysis, J.Z., J.D. and C.T.; writing—original draft preparation, S.W., C.T. and J.Z.; writing—review and editing, S.W., Y.F., C.T., J.D. and G.L.. All authors have read and agreed to the published version of the manuscript.

Funding

This research was funded by Natural Science Basic Research Program of Shaanxi, grant number Program No. 2022JC-23, Innovation Capability Support Program of Shaanxi, grant number Program No. 2023-CX-TD-38.

Availability of data and materials

Data are contained within the article.

Declarations**Competing interest**

The authors declare no conflict of interest.

Received: 26 January 2024 Accepted: 25 February 2024

Published online: 04 March 2024

References

- Anderson D (2004) Eurocode 4 Design of composite steel and concrete structures [J]. Springer Berlin Heidelberg. https://doi.org/10.1007/978-3-642-41714-6_51757
- Classen M (2018) Limitations on the use of partial shear connection in composite beams with steel T-sections and uniformly spaced rib shear connectors [J]. *J Constr Steel Res* 142:99–112. <https://doi.org/10.1016/j.jcsr.2017.11.023>
- Deng WQ, Hu JW, Liu D, Zhao XB, Cha S, Zhang JD (2022) Test and calculation method of shear bearing capacity of cluster welding nail connectors [J]. *China J highway Transp* 35:194–204. <https://doi.org/10.19721/j.cnki.1001-7372.2022.10.018>
- Ding FX, Yin GA, Wang HB (2017) Static behavior of nail connectors in bi-direction push-off tests[J]. *Thin-Walled Structures* 120:307–318. <https://doi.org/10.1016/j.tws.2017.09.011>
- Ding JG, Zhu JS, Kang JF, Wang XC (2021) Experimental naily on grouped nail shear connectors in precast steel-UHPC composite bridge[J]. *Eng Struct* 242:112479. <https://doi.org/10.1016/j.engstruct.2021.112479>
- Fang ZC, Fang HZ, Huang JX, Jiang HB, Chen GF (2022) Static behavior of grouped nail shear connectors in steel–precast UHPC composite structures containing thin full-depth slabs[J]. *Eng Struct* 252:113484. <https://doi.org/10.1016/j.engstruct.2021.113484>
- GB 50917–2013 (2013) Code for Design of Steel-concrete Composite Bridges [S]. China Architecture and Construction Press, Beijing
- GB/T 10433–2002 (2003) Cylindrical head welding nail for arc nail welding [S]. State Administration of Quality Supervision, Inspection and Quarantine, Beijing
- Huang CP, Zhang ZX, Zheng ZJ (2015) Force characteristics and failure mechanism experimental study of group nail in steel concrete composite structure[J]. *J Wuhan Univ Technol* 37:100–105. <https://doi.org/10.3963/j.issn.1671-4431.2015.02.019>
- Li M (2015) Study on refined calculation method and time-effect characteristics of stud connectors of steel-concrete composite beam bridge [D]. Doctoral thesis, Southeast University, Nanjing, China
- Li CJ (2017) Naily on force transfer mechanism and calculation method of shear connectors of assembled composite beams [D]. Doctoral thesis, Chongqing Jiaotong University, Chongqing, China
- Lian WR (2015) Naily on mechanical properties and design method of steel-concrete composite pylon anchorage system with steel anchor box [D]. Doctoral thesis, Chang'an University, Xian, China
- Lin ZF, Liu YQ (2015) Model experiment on shear-tension interaction relation ship of headed studs [J]. *China J Highway Trans* 28:80–86. <https://doi.org/10.19721/j.carolcarrollnki.1001-7372.2015.01.011>
- Luo YZ (2008) Research on bolt-nailed shear joints of steel-concrete composite beams [D]. Doctoral thesis, Central South University, Changsha China
- Okada J, Yoda T, Lebet JP (2006) A naily of the grouped arrangement of nail connectors on the shear strength behavior [J]. *J Struct Mech Earthquake* 23:75–89. <https://doi.org/10.2208/jscseee.23.75s>
- Shi L (2021) Naily on the mechanical behavior of assembled discrete group nail shear key in composite beam [D]. Chongqing Jiaotong University, Chongqing, China, Thesis
- Shi L, Fan L (2022) Experimental naily on mechanical behavior of prefabricated multi-key shear keys [J]. *J Civil Environ Engin* 44:105–112. <https://doi.org/10.11835/JISSN.2096-6717.2020.194>
- Su QT, Han X, Ren F (2014) Mechanical properties of multi-row push-out test specimens [J]. *J Tongji Univ, China* 42:1011–1016. <https://doi.org/10.3969/j.issn.0253-374x.2014.07.004>
- Tong GS. Stability interpretation of multi-storey frame-support frame in GB50017–2017 "Steel Structure Design Standard" [J]. *Steel structure* 2019;3. <https://doi.org/10.13206/j.jgg201901017>
- Tong LW, Chen LH, Wen M, Xu C (2020) Static behavior of nail shear connectors in high-strength-steel-UHPC composite beams. *Eng Struct* 218:110827. <https://doi.org/10.1016/j.engstruct.2020.110827>
- Wang YH, Yu J, Liu JP, Chen YF (2019a) Shear behavior of shear nail groups in precast concrete decks. *Eng Struct* 187:73–84. <https://doi.org/10.1016/j.engstruct.2019.02.002>
- Wang JQ, Qi JN, Tong T, Xu QZ, Xiu HL (2019b) Static behavior of large nail shear connectors in steel-UHPC composite structures. *Eng Struct* 178:534–542. <https://doi.org/10.1016/j.engstruct.2018.07.058>

- Wang W, Zhang XD, Ding FX, Zhou XL (2021a) Finite element analysis on shear behavior of high-strength bolted connectors under inverse push-off loading. *Energies* 14:479. <https://doi.org/10.3390/en14020479>
- Wang W, Zhang XD, Zhou XL, Wu L, Zhu HJ. Nail on Shear Behavior of Multi-Bolt Connectors for Prefabricated Steel-Concrete Composite Beams. *Frontiers in Materials*. 2021 8:2296–8016. <https://www.frontiersin.org/articles/10.3389/fmats.2021.625425>
- Wei X, Xiao L, Wen ZY (2021) Research progress of steel-concrete composite bridge in 2020 [J]. *J Civil Environ Engin* 43:107–119. <https://doi.org/10.11835/j.issn.2096-6717.2020.106>
- Xu C, Sugiura K (2013) FEM analysis on failure development of group studs shear connector under effects of concrete strength and stud dimension [J]. *Eng Fail Anal* 35:343–354
- Xu C, Sugiura K, Wu C, Su QT (2012) Parametrical static analysis on group nails with typical push-out tests[J]. *J Constr Steel Res* 72:84–96. <https://doi.org/10.1016/j.jcsr.2011.10.029>
- Xu H, Zhang S, Rong B (2022) Investigation on shear behavior of nails and PBL shear connectors in steel-concrete hybrid bridge girder. *Structures* 43:1422–1435. <https://doi.org/10.1016/j.istruc.2022.07.050>
- Yang F, Liu Y, Jiang Z (2018) Shear performance of a novel demountable steel-concrete bolted connector under static push-out tests[J]. *Eng Struct* 160:133–146. <https://doi.org/10.1016/j.engstruct.2018.01.005>
- Yu YL, Guo SJ, Wang LC, Yang Y, Xiang YQ (2020) Experimental and numerical analysis of grouped nail shear connectors embedded in HFRCC[J]. *Constr Build Mater* 242:118197. <https://doi.org/10.1016/j.conbuildmat.2020.118197>
- Zhang Q, Jia D, Bao Y (2018) Internal force transfer effect-based fatigue damage evaluation for PBL shear connector groups[J]. *J Constr Steel Res* 148:469–478. <https://doi.org/10.1016/j.jcsr.2018.06.016>
- Zhang J, Hu XM, Fu WJ, Du H, Sun QM, Zhang Q (2020) Experimental and theoretical nail on longitudinal shear behavior of steel-concrete composite beams[J]. *J Constr Steel Res* 171:106144. <https://doi.org/10.1016/j.jcsr.2020.106144>
- Zhang G, Li XY, Tang CH, Song CJ, Ding YH (2023a) Behavior of steel box bridge girders subjected to hydrocarbon fire and bending-torsion coupled loading [J]. *Eng Struct* 296:116906. <https://doi.org/10.1016/j.engstruct.2023.116906>
- Zhang G, Tang CH, Li XY (2023b) Fire resistance of steel truss-concrete composite bridge girder. *J Building Struct* 44:214–226. <https://doi.org/10.14006/j.jzjgxb.2022.0260>
- Zhang AP (2021) Study on shear Performance of stud connectors of Steel-hybrid structure [D]. Doctoral thesis, Zhejiang university, Hangzhou, China
- Zhou XH, Zhi WR, Di J (2014) Nail effect and calculation method of shear bearing capacity of bolted shear connectors of steel anchor box [J]. *J China Highway* 27:13 [JournalArticle/5b435873c095d716a4c7387e](https://doi.org/10.14006/j.jzjgxb.2022.0260)

Publisher's Note

Springer Nature remains neutral with regard to jurisdictional claims in published maps and institutional affiliations.